Electrical Power and Energy Systems 43 (2012) 1144–1154

Contents lists available at SciVerse ScienceDirect

Electrical Power and Energy Systems

journal homepage: www.elsevier.com/locate/ijepes

An autonomous hybrid energy system of wind/tidal/microturbine/battery storage

S.M. Mousavi G. *

Centre of Excellence for Railway, School of Railway Engineering, Iran University of Science and Technology, Tehran, Iran

ARTICLE INFO

Article history:
Received 18 March 2010
Received in revised form 26 April 2012
Accepted 26 May 2012
Available online 15 July 2012

Keywords:
Wind turbine
Tidal turbine
Microturbine
Battery storage
Adaptive control
Supervisory control

ABSTRACT

This paper focuses on dynamic modeling, simulation, control and energy management in an isolated integrated power generation system consisting of a 315 kW offshore wind turbine, a 175 kW tidal turbine, a 290 kW microturbine, and a 3.27 kAh lead acid battery storage. A first, due to efficient and economical utilization of the renewable energy resources, optimal sizing of the hybrid system is accomplished based on economic analysis using genetic algorithms. A model of power-consumption for a microturbine is obtained using least square estimation algorithm based on capstone™ company data and is suggested for implementing at economic analysis. For extraction of maximum energy from a variable speed wind turbine, a developed Lyapunov model reference adaptive feedback linearization method accompanied by an indirect space vector control is applied. Because of more reliability, more fuel flexibility, less environmental pollution, less noise generation and less power fluctuation in comparison with a diesel generator, a microturbine integrated with battery storage is suggested as a back up for this system.

A supervisory controller is designed for energy management between the maximum energy captured from the wind turbine and consumed energies of the load, dump load, energy of the battery based on state of charge and generated energy by the microturbine. Dynamic modeling and simulation are fulfilled using MATLAB Simulink™7.2.

1. Introduction

Renewable energy resources are energies generated from natural resources such as wind, sunlight, tide, hydro, biomass, and geothermal which are naturally replenished. Energy crisis, climate changes such as rise of atmosphere temperature due to increase of greenhouse gases emission and the Kyoto Protocol restrictions in generation of these gases, coupled with high oil prices, limitation and depletion of fossil fuels reserves make renewable energies more noticeable.

Among the renewable energy resources, wind power has had the world's fastest growing energy source (at the rate of 30% annually) in many developed and developing countries over the last 20 years [1]. Active and reactive power control of fixed speed turbines is described in [2,3]. The variable speed wind turbine (VSWT) is used for more attraction of energy from the wind. The VSWT attracts 10–15% more energy, has lower mechanical stress and less power fluctuation in comparison with the fixed speed ones.

One of the most important studies in the VSWT is to apply various control schemes for several purposes in the plant. There are some methods for control of the VSWT. These methods are used to extract the maximum power, to control the voltage and frequency of the load and reduce power fluctuation [4–6]. Maximum power attraction from the VSWT is achieved using linear control; fuzzy logic control and hill climb searching (HCS) method [7–11].

Due to efficient and economical utilization of renewable energies, some of renewable energy resources such as wind turbine and solar array are integrated together and produced excess energy is utilized to store in a battery storage discussed in [12–15]. Because of dependency on wind speed and sun irradiance in such a system, its reliability for satisfying the load demands decreases under all conditions. Hence, some studies propose to use combination of a diesel generator as a back up for these hybrid power generation systems [16–18]. But a diesel generator has several major disadvantages such as low flexibility to respond the demand changes, high pollution and noise, low efficiency. These mentioned problems cause that a diesel generator is not propounded for integration with the clean power generation system.

Another element that plays an important role in an autonomous wind–solar hybrid power generation system is battery storage. Batteries are employed to store superfluous energy derived from wind blowing and solar irradiance during windy or sunny days and then to release during cloudy days or at nights. An ignored aspect in several previous researches is a suitable estimation method of the SOC of the battery for the appropriate management of energy in the hybrid power generation systems. So far, several SOC estimation methods are employed for a battery such as fuzzy logic, neural network, and specific gravity measurement; open circuit voltage estimation, Kalman/extended Kalman filters and Ampere-hour

* Tel.: +98 2177491029 30; fax: +98 2177451568.
E-mail address: sm_mousavi@iust.ac.ir

0142-0615/$ - see front matter © 2012 Elsevier Ltd. All rights reserved.
http://dx.doi.org/10.1016/j.ijepes.2012.05.060

counter [19–21]. One of these methods will be utilized for the hybrid system.

One of the most important studies in a hybrid system is economic analysis and size optimization in order to achieve efficient and economical utilization in the hybrid system. Various methods and techniques such as a graphic construction technique, design space approach, genetic programming (GA), and dynamic programming are implemented for economical analysis and size optimization in various hybrid systems such as wind/solar/battery storage, and wind/solar/diesel/battery considered in [22–27]. As a result of robust in finding global optimal solutions, the GA technique is implemented for optimal sizing design of the hybrid system in this study.

Renewable energy sources have unique characteristics which influence where they are used. Generally, solar energy can be applied in areas where the amount of sun irradiance is sufficient. Areas where winds are stronger such as offshore sites are preferred locations for wind turbines. Furthermore, energy in water can be used. Since water density is about 1000 times more than air, even a slow flowing stream of water can be utilize to produce considerable amounts of energy. These cause that integration of wind turbine, tidal turbine, microturbine, and battery storage is proposed to utilize in the area with above specification such as in an oil platform. Utilization of a microturbine as a back up in the hybrid system makes higher reliability, less power fluctuation, less environmental pollution and less noise generation. For example, a traditional 30 kW diesel generator emits more nitrogen oxide in one hour than a Capstone unit does in more than nine days of full-load operation [28].

Because of nonlinear behavior of the plant, the methods based on linear control theory, such as a proportional integral derivative (PID) controller, are not suitable for the maximum power point tracking (MPPT). The maximum energy attraction and voltage and frequency control of the load are performed using fuzzy logic control method. Generally, a fuzzy logic controller does not guarantee an optimal response. Furthermore, it increases complexity of the control system. The MPPT using the HCS method is appropriate only for the wind turbines with quite small inertia. For the wind turbines with large inertia, this method is not able to extract the maximum power. Thus, the input–output feedback linearization method is proposed to eliminate the nonlinear behavior of the plant. Model reference adaptive control method is used to estimate the plant parameters such as optimum torque and rotor angular speed in order to capture the maximum energy from the VSWT when the wind speed change.

For proper performance of central controller, a suitable SOC estimation method is needed in order to generate the reference values for the controllers in the hybrid system. Among the SOC estimation methods, the Kalman filter, neural network and fuzzy logic are very complex and also too much calculations must be executed. In the specific gravity method, the electrolyte may become laminated and leads to diminish the sensors lifetime. A dynamic mathematical model of a lead acid battery proposed by Matthias Durr et.al in [29] is used for this hybrid system. Based on the remaining battery energy, a new value for the battery open circuit voltage is determined using the look-up table. The SOC calculation is expressed in a look-up table relative to the battery open circuit voltage (V_{OC}).

An appropriate supervisory controller is designed for energy management between maximum energy captured from the wind turbine/tidal turbine and consumed energies of the load, dump load, battery energy based on state of charge and the energy generated by the microturbine. This paper is organized as follows: Description of the proposed system is presented in Section 2. Section 3 describes the control system design. Optimal design and economic analysis is fulfilled in Section 4. Simulation results and discussion are presented in Section 5. Section 6 is the conclusions.

2. Proposed system description

The proposed hybrid energy generation system is depicted in Fig. 1. This system consists of a wind turbine, a microturbine, a battery storage, induction and synchronous generators, indirect space vector control (ISVC) scheme, sinusoidal pulse width modulation (SPWM) converters, dc/dc converters, an adaptive feedback linearization controller, load, dump load and a supervisory controller.

2.1. Wind energy conversion system

Every wind energy conversion system (WECS) consists of two or three blades, Pitch angle control mechanism, yaw mechanism, gearbox, generator and converters. A squirrel cage induction generator (SCIG) [30], a doubly fed induction generator [31] and a permanent magnetic synchronous generator [32] are used in the WECS. The SCIG is chosen to be used in this system because of its simple and robust mechanical structure. Stator is connected to the load via converters. The dynamic modeling of the squirrel cage induction generator in a stationary dq0 reference frame is demonstrated as following in [33].

Rectifier and inverter used in the WECS are pulse width modulation (PWM) controlled converters (AC/DC/AC). Some researchers implement the AC/AC converter [34]. A six-pulse- full-controlled rectifier is used to convert the AC output of self excited induction generator (SEIG) into DC voltage. Voltage source inverter (VSI) using pulse width modulation topology is implemented to convert the dc link voltage to ac output voltage [35]. It consists of six insulated gate bipolar-junction transistors (IGBT). Furthermore, the SPWM is used in order to generate the gating pulse for applying to the IGBT. The reference signal in the gating circuit for the IGBTs in each leg is displaced by 120° achieved by shifting the reference signal of the PWM. By comparing a sinusoidal reference voltage with a triangular waveform, the gating signals are created. In the basic operation of the circuit, if the sinusoidal voltage is higher than the triangular waveform, the output of the comparator will be one; otherwise the output will be zero.

The output power and torque of turbine (T_t) vs. rotational speed in the WECS are given as follows:

$$P_w = \frac{1}{2}\rho \cdot A \cdot C_p(\lambda,\beta)\left(\frac{R\cdot\omega_{opt}}{\lambda_{opt}}\right)^3 \tag{1}$$

$$T_t = \frac{1}{2}\rho \cdot A \cdot C_p(\lambda,\beta)\left(\frac{R}{\lambda_{opt}}\right)^3 \cdot \omega_{opt}^2 \tag{2}$$

Furthermore, the output power of a wind turbine vs. wind speed is approximated by an equation as follows [26]

$$P_w(V) = \begin{cases} \frac{V^2 - V_{cin}^2}{V_{rat}^2 - V_{cin}^2}\cdot P_r; V_{cin} \leqslant V \leqslant V_{rat} \\ P_r; V_{rat} \leqslant V \leqslant V_{cout} \\ 0; V \leqslant V_{cin} and V \geqslant V_{cout} \end{cases} \tag{3}$$

where P_r, V_{cin}, V_{rat} and V_{cout} are the rated power, the cut-in wind speed, the rated wind speed and the cut-off wind speed, respectively.

The power coefficient is maximized for an optimum TSR value when the blade pitch angle is zero. The optimum rotor speed can be calculated as following equations:

$$\omega_{opt} = \frac{\lambda_{opt}}{R}\cdot V_{wn} \tag{4}$$

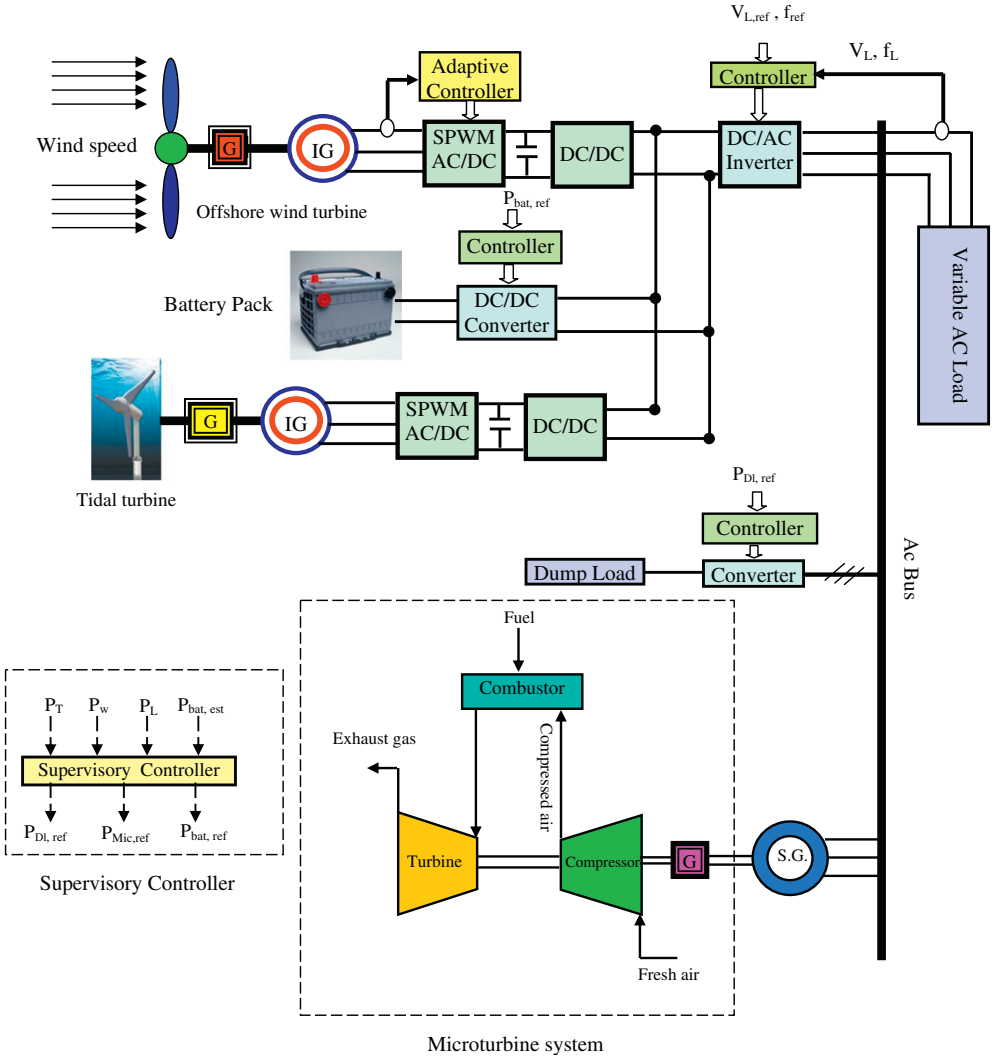

Fig. 1. The proposed hybrid system structure.

Thus

$$V_{wn} = \frac{R \cdot \omega_{opt}}{\lambda_{opt}} \tag{5}$$

where ω_{opt}, λ_{opt}, R, and V_{wn} are optimum rotor angular speed (rad/s), optimum tip speed ratio, radius of turbine blade (m) and wind speed (m/s), respectively. For the WECS, power coefficient (C_P) is maximized for an optimum TSR value when the blade pitch angle is zero.

2.2. Tidal turbine

Tidal power is captured using tidal turbines. Tidal powers are more predictable than wind and solar powers. Tidal stream and tidal barrage are two different classifications for generating energy from the tides. The kinetic energy of moving water and the potential energy in height are used in tidal stream and tidal barrage system, respectively. The energy captured from tidal stream system that is suitable for integrating with the proposed WECS can be expressed as

$$P_T = \frac{1}{2}\rho \cdot A \cdot C_{pt}(\lambda, \beta) \cdot V_t^2 \tag{6}$$

where ρ is the density of water (approximately 1000 kg/m^3), A the swept turbine area (m^2), C_{pt} the turbine power coefficient and V_t is the velocity of water flow. The operation of tidal energy conversion system (TECS) is similar to the WECS in modeling and output response with distinction that the speed of water fluid is much less than the air fluid [36].

2.3. Microturbine model

A microturbine is a small high-speed gas turbine that generates electrical power within 20–500 kW range. It consists of four components: compressor, combustor, turbine and generators. Single- and split-shaft are two types of microturbines. In the single-shaft microturbine, the turbine and generator are mounted on the same shaft. Output frequency of the microturbine is from about 400 Hz up to several kilo Hertz. It must be converted to 60 Hz using power electronic converters. In the spilt-shaft configuration, implemented in this paper, the turbine shaft is connected to the generator by a gearbox and the converters are not needed [37–39]. The GAST model, developed by General Electric, is one of the most commonly model to simulate a gas turbines [40]. The model configuration of the microturbine is shown in Fig. 2.

2.4. Battery storage model

The battery storage accompanied by the microturbine is used as a backup for the wind energy conversion system. The value of each

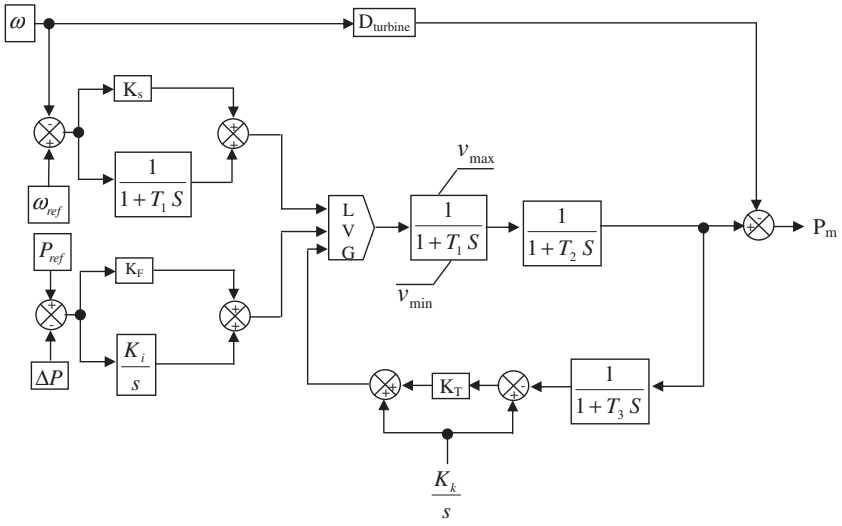

Fig. 2. Implemented model of microturbine.

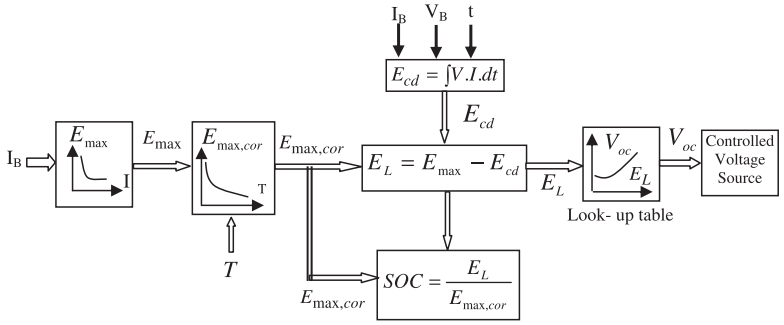

Fig. 3. Block diagram for determining V_{oc} and SOC.

element is functions of open circuit voltage (V_{oc}) and state of charge (SOC) [29]. V_{oc} depends on battery discharge current (I_B), attracted energy from battery (E_{cd}) and battery temperature (T_b). In this model, battery remained energy for determining V_{oc} is calculated using a look up table. Fig. 3 shows the algorithm of block diagram for determining the V_{oc} and SOC. In this model, the battery initial current is used to estimate the maximum available energy. For determining the remainder energy of the battery and SOC, the energy being drawn from the battery is dynamically calculated and subtracted from the initial energy.

3. Control systems design

The most important objectives of the control systems used in this paper are: (i) capturing the maximum power from the wind turbine using the ISVC scheme and adaptive feedback linearization method; (ii) control of the load voltage and frequency using a SPWM voltage source inverter (SPWM-VSI) control and (iii) energy management between generated and consumed energies of the hybrid system components using the supervisory controller.

3.1. Indirect space vector, feedback linearization and developed model reference adaptive controllers design

3.1.1. Indirect space vector controllers design

In this section, voltage and current of the stator are controlled by the stator indirect space vector control based on stator field *dq*0 model. The equations of electromagnetic torque of the induction generator are discussed in [35].

$$T_{eg} = \frac{3P}{4}\frac{L_m}{L_r}\cdot(i_{qs}\cdot\lambda_{dr} - i_{ds}\cdot\lambda_{qr}) \tag{7}$$

$$\lambda_{qr} = \frac{L_m}{1+\frac{L_r}{r_r}\cdot S}\cdot i_{qs} \tag{8}$$

$$i_{ds} = -\frac{4}{3P}\cdot\frac{L_r}{L_m}\cdot\frac{T_{em}}{\lambda_{qr}} \tag{9}$$

$$\omega_{sl} = -\frac{L_m}{L_r}\cdot\frac{r_r}{\lambda_{qr}}\cdot i_{ds} \tag{10}$$

where r_r, L_r i_d, i_q, v_d, v_q, λ_d and λ_q are rotor winding resistor, rotor inductance, currents, voltages and fluxes of the d-q model, respectively.

The optimum torque ($T_{ae,opt}$) obtained using adaptive controller is used as input of ISVC. i^*_{qs} and i^*_{ds} are obtained using the $T_{ae,opt}$ and the ISVC equations. Furthermore, v^*_{ds} and v^*_{qs} are generated by controllers based on these currents. v^*_a, v^*_b and v^*_c are obtained from these voltages using *dq*0/*abc* converter based on reference signals for sinusoidal pulse width modulation generator to generate pulses for applying to the IGBT gates of rectifier.

3.1.2. Feedback linearization and developed model reference adaptive controllers design

The input–output linearization method is used for obtaining a linear relationship between a new input (μ) and the output (y) [42]. Fig. 4 shows the driven train of the SEIG. In this figure, K_{ls}, B_{ls}, J_r, K_r, ω_r, J_g, K_g and ω_g are the shaft damping, the shaft stiffness, the rotor inertia, the rotor external damping, the rotor angular seed, the inertia, the external damping and the angular speed of

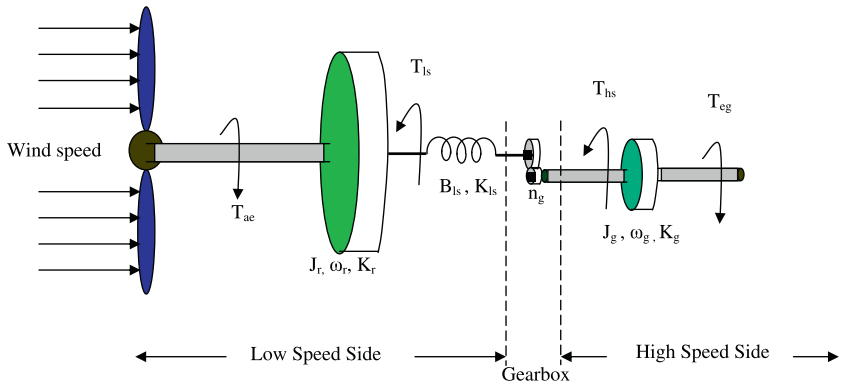

Fig. 4. Driven train of the SEIG.

the generator, respectively. Also, T_{ae} is the aerodynamic torque, T_{ls} the low speed shaft torque, T_{hs} the high speed shaft torque, T_{eg} the electromagnetic torque of generator and n_g is the gearbox coefficient. The dynamic equations for the low speed shaft and the high speed shaft are [41]

$$T_{ls} = K_{ls} \cdot (\omega_r - \omega_{ls}) + B_{ls} \cdot (\theta_r - \theta_{ls}) \tag{11}$$

$$T_{hs} = n_g \cdot T_{ls} \tag{12}$$

Relationship between the rotor angular speed (ω_r), the aerodynamic and the electromagnetic torques can be written as [41]

$$J\frac{d\omega_r}{dt} + K \cdot \omega_r = T_{ae} - T_{eg} \tag{13}$$

$$K = K_r + n_g^2 \cdot K_g \tag{14}$$

Assuming μ is an additional input and T_{ae} is an aerodynamic estimation of the wind turbine torque; μ is given as

$$\mu = \frac{\widehat{T}_{ae} - T_{eg}}{J} - \frac{K}{J}\omega_r \tag{15}$$

Thus, the generator torque is written

$$T_{eg} = J \cdot \left(\frac{\widehat{T}_{ae}}{J} - \mu\right) - K\omega_r \tag{16}$$

This leads to the following equation

$$J\frac{d\omega}{dt} + K \cdot \omega_r = T_{ae} - \left(J \cdot \left(\frac{\widehat{T}_{ae}}{J} - \mu\right) - K\omega_r\right) \tag{17}$$

Consequently

$$\frac{d\omega}{dt} = \frac{T_{ae} - \widehat{T}_{ae}}{J} + \mu = \frac{\widetilde{T}_{ae}}{J} + \mu \tag{18}$$

If $\widetilde{T}_{ae}$ becomes zero, then the Eq. (18) can be written

$$\frac{d\omega}{dt} = \mu \tag{19}$$

For the aerodynamic estimation, the optimum rotor angular speed is written using Eq. (4) as

$$\omega_{opt} = n\frac{\lambda_{opt}}{R}v_{wn} \tag{20}$$

If $e$is the tracking error

$$e = \omega_{opt} - \hat{\omega}_r \tag{21}$$

The dynamic error at closed loop system can then be expressed with

$$\frac{de}{dt} + a_0 e = 0 \tag{22}$$

Using Eqs. (19), (21) and (22) is obtained

$$\mu = \frac{d\omega_{opt}}{dt} + a_0 \cdot e \tag{23}$$

a_0 is the designed parameter. According to a model reference adaptive system (MRAS) [43]

$$e(t) = H(p) \cdot [K \cdot \phi^T(t) \cdot \mu(t)] \tag{24}$$

where e is the scalar error, $H$is the strictly positive real transfer function and ϕ is the vector function of time. The variation of $\phi(t)$ is defined as [40,42]

$$\frac{d\phi(t)}{dt} = \eta \cdot e \cdot \mu(t) \cdot sgn(K) \tag{25}$$

$\eta$is a positive constant. Assuming μ is bounded

If $t \to \infty$ then $e(t) \to 0$

According to the previous equations, the following adaptive relation for $\widehat{T}_{ae}$ is suggested

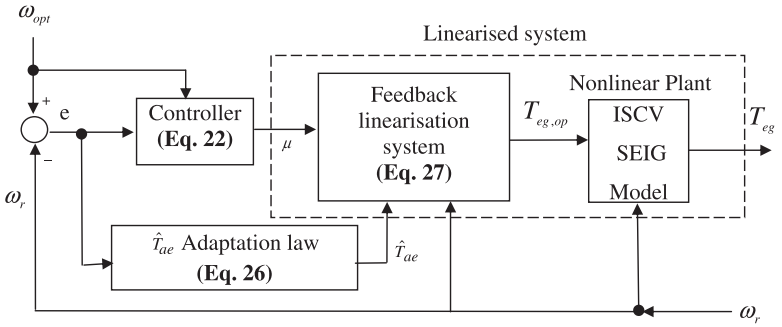

Fig. 5. Configuration of the adaptive feedback linearization controller.

$$\widehat{T}_{ae} = \frac{\eta \cdot e}{J} \tag{26}$$

Then the optimum torque ($T_{ae,opt}$) is obtained

$$T_{eg,opt} = \widehat{T}_{ae} - J \cdot \mu - K \cdot \omega_r \tag{27}$$

Configuration of the adaptive feedback linearization controller is shown in Fig. 5. It is implemented to design of linear controller. It causes that the linear PID controller is encountered with a linear plant instead of a nonlinear one. Thus, the design of the PID controller is fulfilled using Ziegler–Nichols method based on Eq. (22). Adaptive controller operates as Eq. (26). This controller generates the estimated torque ($\widehat{T}_{ae}$) based on difference between the rotor angular speed and optimum angular speed ($\omega_{opt} - \omega_r$). The feedback linearization makes a linear relationship between input and output of the plant according to Eq. (27).

3.2. Supervisory controller

For management of the maximum energy captured from the WECS and TECS, a supervisory controller is applied. After adjusting the WECS for the maximum energy generation using the adaptive feedback linearization controller, the supervisory controller calculates the reference powers for the battery regulator controller, microturbine controller and dump load controller based on subtraction of the load power from the wind/ tidal turbines powers ($P_e = P_w + P_T - P_L$) according to the flow chart shown in Fig. 6. In the flowchart; P_w, P_T, $P_{b,est}$, $P_{b,ref}$, $P_{dl,ref}$, $P_{MT,ref}$ and P_e are the maximum power extracted from the wind turbine, tidal turbine, estimated battery power calculated dynamically using the method discussed in Section 2.4, battery reference power, dump load reference power, microturbine reference power and excess/deficiency power calculated based on subtraction between generated and consumed energies, respectively.

All steps of the supervisory controller operation in the flow chart are explained as below:

- Step 1: compare the wind/tidal turbines generated powers with the load power ($P_e = P_w + P_T - P_L$), if P_e is positive, go to step 2, otherwise go to step 7.
- Step 2: The battery is in charge mode. Rapid charge is applied for charging the battery so that it is charged at an hour. In this step, P_e is positive, this means that generated sum of wind turbine and tidal turbines powers is more than load power; if the estimation of battery power ($P_{b,est}$) is equal to the maximum charge power go to step 3, otherwise go to step 5.
- Step 3: In this step, P_e is positive, if the excess power is less than the maximum charge power, apply $P_{b,ref} = P_e$, otherwise; calculate $\Delta P_2 = P_e - 100$ and go to step 4.
- Step 4: If $\Delta P_2 = 0$, apply $P_{b,ref} = 100$ kW, otherwise; apply $P_{b,ref} = 100$ kW and $P_{dl,ref} = \Delta P_2$.

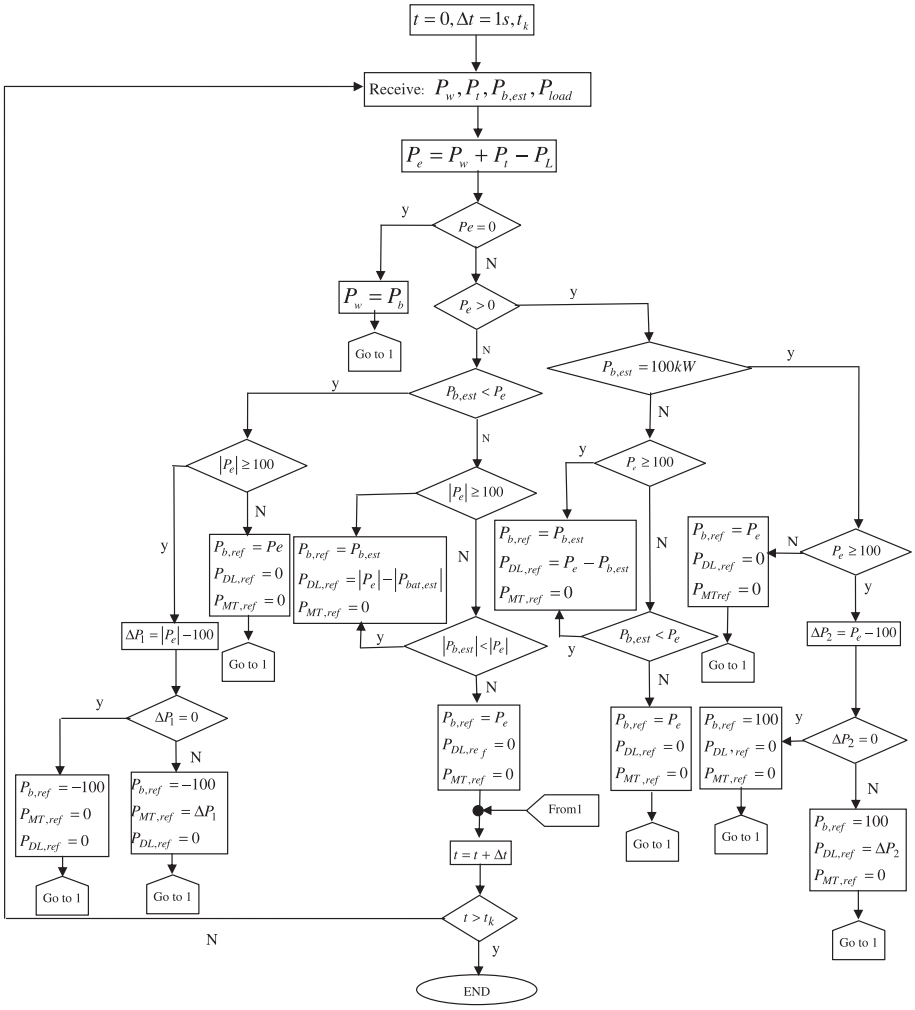

Fig. 6. Supervisory controller operation flow chart.

Step 5: In this step, P_e is positive, if the excess power is more than the maximum charge power apply $P_{b,ref} = P_{b,est}$ and $P_{dl,ref} = P_e - P_{b,est}$, otherwise; go to step 6.
Step 6: If $P_{b,est} \prec P_e$, go to step 5, otherwise apply $P_{b,ref} = P_e$.
Step 7: In this step, P_e is negative, this means that the wind/tidal generated powers is less than load power; if the battery discharge power estimation is less than the power deficiency, go to step 8, otherwise; go to step 10.
Step 8: In this step, P_e is negative, if the absolute value of the power deficiency is less than the absolute value of the maximum discharge power (−100 kW), apply $P_{b,ref} = P_e$, otherwise calculate $\Delta P_1 = |P_e| - 100$ and go to step 9.
Step 9: If ΔP_1 is zero, apply $P_{b,ref} = -100$ kW, otherwise apply $P_{b,ref} = -100$ kW and $P_{MT,ref} = \Delta P_1$.
Step 10: In this step, P_e is negative, if the absolute value of the power deficiency is more than the absolute value of the maximum discharge power apply $P_{b,ref} = P_{b,est}$ and $P_{MT,ref} = |P_e| - |P_{b,est}|$, otherwise go to step 11.
Step 11: If the absolute value of the battery estimated power is less than the absolute value of P_e, go to step 10, otherwise apply $P_{b,ref} = P_e$.

4. Optimal sizing and economic analysis

The main purpose of this section is to find the optimal size of a stand-alone wind turbine/tidal turbine/microturbine/battery storage system utilized to satisfy the requirements of given load demands base on economical analysis. Among several techniques and methods used to achieve the optimal configurations of hybrid systems, genetic algorithms method is implemented because of its robust in finding global optimal solutions and particularly in multimodal optimization problems. For economical analysis and optimal design of the hybrid system, Total annualized cost of system (ACS) composed of annualized capital cost (C_{acap}), annualized replacement cost (C_{arep}), annualized operation and maintenance cost ($C_{ao\&m}$), and annualized fuel cost ($C_{a\ fuel}$) for five main parts, consist of wind turbine, microturbine (MT), tidal turbine, battery storage and the other devices included controller, inverter, rectifier and chopper, are considered [26].

$$\begin{aligned} ACS = {} & C_{\text{acap}}(\text{wind Turbine} + \text{Tidal turbine} + \text{MT} + \text{Battery} \\ & + \text{others}) + C_{\text{arep}}(\text{battery}) + C_{\text{ao\&m}}(\text{wind Turbine} \\ & + \text{Tidal turbine} + \text{MT} + \text{Battery} + \text{others}) \\ & + C_{\text{afuel}}(\text{MT}) \end{aligned} \tag{28}$$

4.1. The annualised capital cost

The annualised capital cost of each component is defined as the following equation [26]

$$C_{\text{acap}} = C_{\text{cap}} \cdot \text{CRF}(\text{i}, \text{Yproj}) \tag{29}$$

C_{cap}, Y_{proj} and CRF are the initial capital cost of each component, the component lifetime, and capital recovery factor respectively. CRF is determined as the following equation [26]

$$CRF(i, Y_{proj}) = \frac{i \cdot (1+i)^{Y_{proj}}}{(1+i)^{Y_{proj}} - 1} \tag{30}$$

i is the annual real interest rate related to nominal interested rate, i', and the annual inflation rate f, as follow

$$i = \frac{i' - f}{1 + f} \tag{31}$$

4.1.1. Annualized replacement cost

The annualized replacement cost (ARC) is defined only for battery storage replaced periodically during the project lifetime. The ARC is calculated as [26]

$$C_{arep} = C_{rep} \cdot SFF(i, Y_{proj}) \tag{32}$$

where, SFF is the sinking fund factor and is stated as [26]

$$SFF(i, Y_{proj}) = \frac{i}{(1+i)^{Y_{proj}} - 1} \tag{33}$$

4.2. Annualized fuel cost

The annualized fuel cost function, $C_{afuel}(MT)$, is just used for microturbine. For obtaining of the cost function of a microturbine, fuel cost curve vs. output power is modeled as the following equation

$$C_{afuel} = \alpha + \beta \cdot P_m + \gamma \cdot P_m^2 \tag{34}$$

If the points of fuel cost curve vs. output power are clarified, the α, β, γ will be determined using least square estimation algorithms.

$$J = \sum_{j=1}^{k} \left(\alpha + \beta \cdot P_{mj} + \gamma \cdot P_{mj}^2 - C_{afuel} \right)^2 \tag{35}$$

$$\partial J / \partial \alpha = \sum_{j=1}^{k} 2 \cdot (\alpha + \beta \cdot P_{mj} + \gamma \cdot P_{mj}^2 - C_{afuel}) = 0 \tag{36}$$

$$\partial J / \partial \beta = \sum_{j=1}^{k} 2 \cdot P_{mj} \cdot (\alpha + \beta \cdot P_{mj} + \gamma \cdot P_{mj}^2 - C_{afuel}) = 0 \tag{37}$$

$$\partial J / \partial \gamma = \sum_{j=1}^{k} 2 \cdot P_{mj}^2 \cdot (\alpha + \beta \cdot P_{mj} + \gamma \cdot P_{mj}^2 - C_{afuel}) = 0 \tag{38}$$

Thus an algebraic equation set vs. α, β, γ is obtained as following

$$k \cdot \alpha + \beta \cdot \sum_{j=1}^{k} P_{mj} + \gamma \cdot \sum_{j=1}^{k} P_{mj}^2 = \sum_{j=1}^{k} C_{afuel} \tag{39}$$

$$\alpha \cdot \sum_{j=1}^{k} P_{mj} + \beta \cdot \sum_{j=1}^{k} P_{mj}^2 + \gamma \cdot P_{mj}^3 = \sum_{j=1}^{k} P_{mj} \cdot C_{afuel} \tag{40}$$

$$\alpha \cdot \sum_{j=1}^{k} P_{mj}^2 + \beta \cdot \sum_{j=1}^{k} P_{mj}^3 + \gamma \cdot P_{mj}^4 = \sum_{j=1}^{k} P_{mj}^2 \cdot C_{afuel} \tag{41}$$

4.3. Annualized operation and maintenance cost

The maintenance cost of the nth year $C_{a\ o\&m}(n)$ is calculated based on the maintenance cost of the first year $C_{a\ o\&m}(1)$ as [26]

$$C_{ao\&m}(n) = C_{ao\&m}(1) \cdot (1+f)^n \tag{42}$$

For minimization of the ACS objective function, the following constraints must be imposed:

$$0 \leqslant P_w \leqslant P_{L,\max} \tag{44}$$
$$0 \leqslant P_T \leqslant P_{L,\max} \tag{45}$$
$$0 \leqslant P_{MT} \leqslant P_{L,\max} \tag{46}$$

Genetic algorithm is a technique implemented in order to find optimized answer in optimization problems. The GA is categorized as global search heuristics that use techniques inspired by evolutionary biology such as inheritance, mutation, selection, and crossover.

Two-point crossover, roulette wheel selection methods have been selected to each chromosome. Gatool is used for the achieving the minimum cost based on obtained cost function. Fitness scaling is Rank, Selection function is Roulette, Crossover function is 0.7,

Mutation function is Uniform 0.2, Crossover is Two point, and Initial population is 50.

5. Simulation results and discussion

MATLAB Simulink™7.2 is used to evaluate the performance of the proposed hybrid power generation system and controllers. The mathematical model and design details of each component in the hybrid power generation system were presented in the previous sections. For the energy conversion system used in this paper, pitch angle is supposed zero and yaw control mechanism is not considered. It consists of aerodynamic system based on wind speed model, wind power vs. wind speed model and etc., induction generator (SEIG), a SPWM AC/DC converter, a DC/DC buck-boost converter, a DC/AC inverter, AC filters, adaptive, PID and ISVC controllers. The Specifications of the induction generator and the SPWM AC/DC converter of the WECS are shown in Tables 1 and 2, respectively. The DC/DC converter is used in order to fix the DC link voltage for the inverter. The specifications of this chopper are given in Table 3.

The microturbine is required for the time that the hybrid system of wind turbine, tidal turbine and battery storage cannot satisfy the load demands. It consists of compressor, combustor, turbine and generator. Mathematical model and the specifications of the synchronous generator used for microturbine are presented in Fig. 2 and Table 4, respectively [39].

Accompanied by the microturbine, the lead acid battery and a boost dc/dc converter are used. The boost converter and a controller are required in order to control the voltage of battery bus based on the battery reference power value ($P_{b,ref}$). The parameters of this converter and controller have been shown in Table 5. In this converter, the IGBT is controlled using a proportional and integral (PI) controller. This controller alters the duty cycles of pulses applied to the chopper IGBT gates. The battery capacity and charge efficiency of the charger are 3.27 kAh and 85%, respectively.

The dump load is used to consume the excess power. It consists of three phase resistors connected in series with gate turned off (GTO) switches. The consumed power by the resistors of the dump load is discussed in [44].

Optimal sizing based on economical analysis, discussed in Section 4, is accomplished using the GA for maximum load demands (400 kW). The cost and lifetime of each component is shown in Table 6. In order to obtain the annualized cost of microturbine, the least square estimation algorithm was applied. For calculation of α, β and γ, the fuel flow input of some microturbine produced by Capstone™ company is implemented that is given in Table 7. The results of this analysis are obtained as: size of 315 kW for wind turbine, 175 kW for tidal turbine, 290 kW for microturbine and 3.27 kAh for lead acid battery. The total cost of this hybrid system based the economical analysis becomes 312,080 $.

There are three models in the wind speed modeling; amongst all, wind guest model is used in this paper. The wind and tidal speeds variations are shown in Fig. 7. The wind speed changes approximately between 7 m/s and 13 m/s. Also, the tidal speed varies between 1.5 m/s and 2.5 m/s. The generated power by the WECS and TECS are shown in Fig. 8. The initial load power is 350 kW. At t = 600 min, the load power increased to 150 kW using a three phase breaker and then at t = 1200 min, the load power decreased up to 350 kW using another three-phase breaker. Furthermore, sum of generated power from wind and tidal turbines and load power are shown in Fig. 9.

According to the wind turbine generated power and the load power profiles, from t = 0 to t = 600 min, generated wind turbine power is less than the load power (350 kW) and the battery will be in discharging mode. But in some subintervals of this duration, the power deficiency is more than the maximum discharge power. In this case, the battery is discharged based on the maximum discharge power; remainder unmet load power is consumed by the microturbine.

Furthermore, in the time duration of t = 600 min to t = 1200 min, the wind turbine generated powers is more than the load power (150 kW) and the battery will be in charging mode. But in some subintervals of this duration, the excess power is more than the maximum charge power. In this case, the battery is charged based on the maximum charge power by dump load in order to prevent

Table 1
Induction generator model parameters for the WECS.

Nominal power	400 kVA
Nominal voltage (line-to-line)	480 V
Nominal frequency	60 Hz
Generator type	Squirrel cage
Stator resistance	0.01615 p.u.
Stator inductance	0.05258 p.u.
Rotor resistance	0.01515 p.u.
Rotor induction	0.05258 p.u.
Mutual induction (L_m)	2.95 p.u.
Inertia constant	1.2 s
Friction factor	0
Pairs of poles	2

Table 2
The SPWM AC/DC converter specifications for the WECS.

Semiconductor switch type	IGBT/DIODE
Snubber resistance	5 kΩ
Snubber capacitor	Inf.
Internal resistance	1 mΩ
Carrier frequency	3 kHz

Table 3
DC/DC converter specifications of the WECS.

Chopper type	Buck-boost
Semiconductor switch type	IGBT
Converter inductor	185 mH
Converter capacitor	1900 μF
Switching frequency	2 kHz
Proportional gain of voltage control system	16.6
Integral gain of voltage control system	7.5
PWM reference voltage	440 V

Table 4
Synchronous specifications of microturbine.

Rated power	380 kW
Rated line to line voltage	660 V
Frequency	60 Hz
Inertia constant (H)	0.822 s
Friction factor	0

Table 5
DC/DC converter specifications of the battery storage.

Chopper type	Boost
Semiconductor switch type	IGBT
Converter inductor	155 mH
Converter capacitor	2500 μF
Switching frequency	2 kHz
Proportional gain of voltage control system	0.15
Integral gain of voltage control system	0.38
PWM reference voltage	440 V

Table 6
The costs and lifetime of each component.

	Initial capital cost	Replacement cost	Fuel cost	Maintenance cost in the first year	Lifetime (year)
Wind turbine	3500 $/kW	Null	Null	90 $/kW	20
Tidal turbine	5200 $/kW	Null	Null	63 $/kW	20
Microturbine	850 $/kW	Null	0.0037 $/kW	85 $/kW	20
Battery storage	1500 $/kAh	1500 $/kAh	Null	50 $/kAh	5
Others	8000 $	Null	Null	80 $	20

Table 7
Characteristics of fuel flow input vs. output power.

Fuel flow input (MBTU/h)	Operational power of microturbines
0.433	25
0.842	60
2.28	190
6.84	500

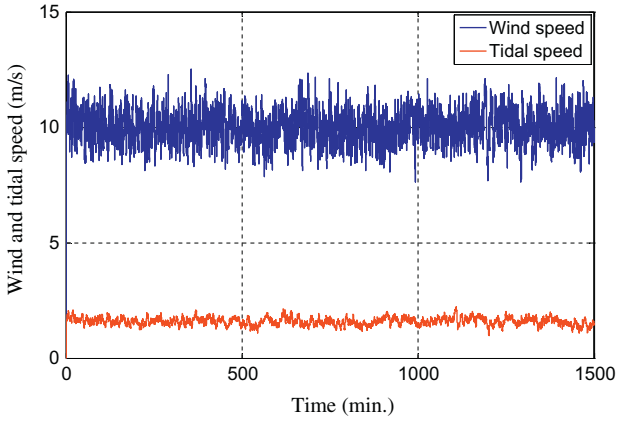

Fig. 7. Wind speed and tidal speed variations.

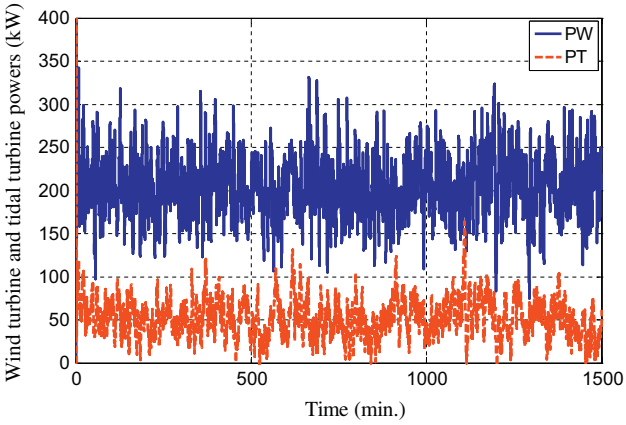

Fig. 8. Power extracted from wind turbine and tidal turbines.

overcharging of the battery. So, the dump load operates as a protector for the battery.

The supervisory controller role is to adjust the reference powers of the microturbine and dump load based on excess and deficiency powers. The operation of the controllers and hybrid system in the other subintervals is similar to the considered durations. The battery power and dump load/ microturbine powers discussed in this section are shown in Figs. 10 and 11, respectively.

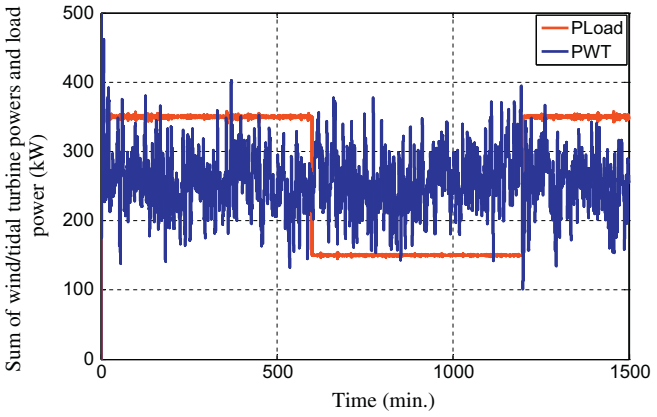

Fig. 9. Load power and sum of extracted powers from wind/tidal turbines.

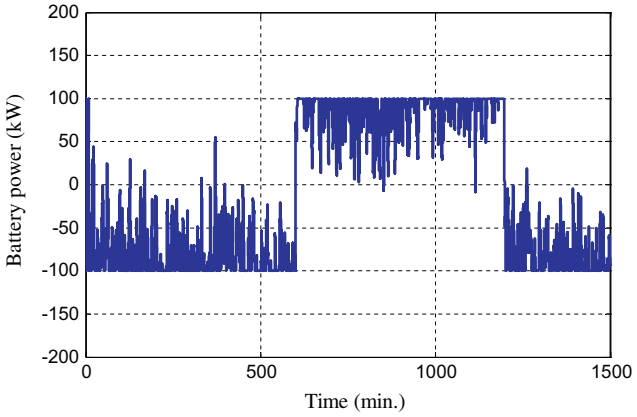

Fig. 10. Battery power in charge or discharge modes.

A DC/AC inverter is utilized to adjust the load voltage and frequency to 230 V and 60 Hz for satisfying the required load power using the SPWM method. The switching frequency of the inverter is 2 kHz. In order to eliminate the switching harmonics, a 5 mH inductive low output passive filter is applied. Specifications of the SPWM inverter are given in Table 8. The line-to-line output voltage amplitude in the SPWM inverter is determined as the following equation [45]:

$$V_{L-L} = \frac{\sqrt{3}}{2\sqrt{2}} \cdot m_a \cdot V_{dc-Link} \tag{47}$$

$V_{dc-link}$ is the DC link voltage and m_a is the amplitude modulation index. According to the Eq. (47), since the amplitude modulation index is 0.85 and the DC link voltage is adjusted to 440 V by the DC/DC converter, the obtained line to line AC voltage of the inverter for satisfying the load demands is approximately 230 V. The profiles of root mean square (RMS) value of the load voltage in per unit (p.u.) system and load frequency (Hz) are evident in Figs. 12 and 13.

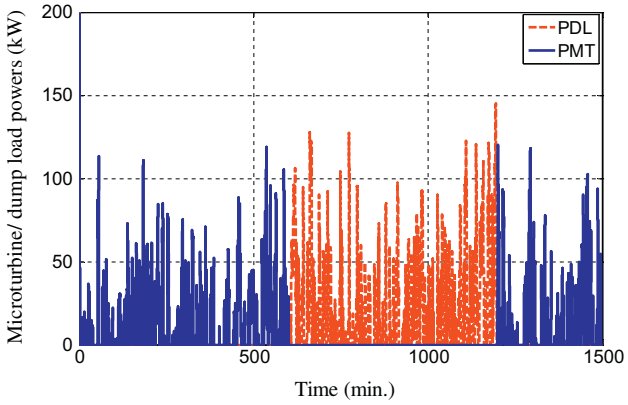

Fig. 11. Microturbine and dump load powers.

Table 8
SPWM DC/AC inverter specifications.

Semiconductor switch type	IGBT/DIODE
Snubber resistance	6.5 kΩ
Snubber capacitor	Inf.
Internal resistance	1 mΩ
Carrier frequency	3 kHz
Modulation index	0.85
Frequency of out put voltage	60 Hz

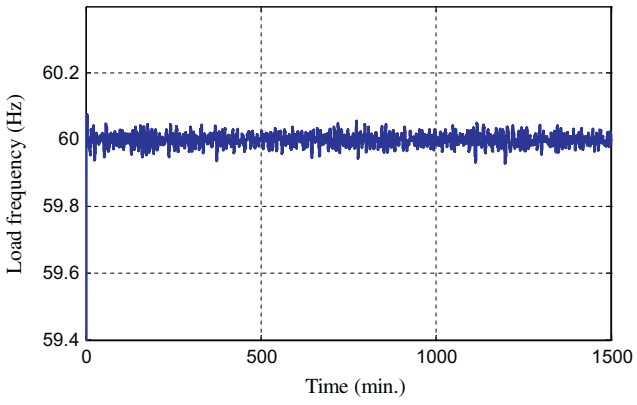

Fig. 12. Load frequency changes.

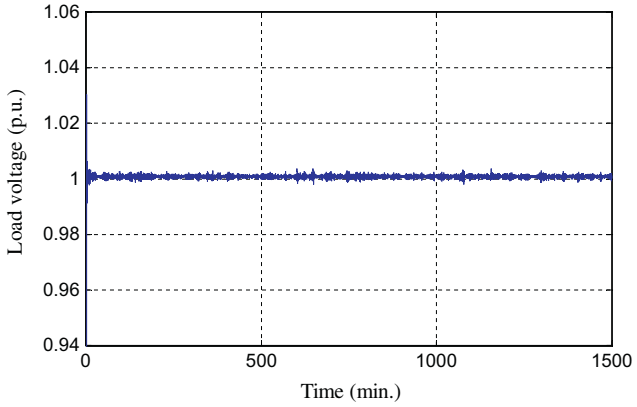

Fig. 13. RMS value of output voltage.

According to these figures, the variation of the RMS value of the load voltage is less than 0.85 % and the variation of the RMS value of the load frequency is less than 0.16 % that are acceptable.

6. Conclusions

In this paper, synthetic operation of an offshore wind turbine, a tidal turbine, a microturbine, and a battery storage working together as autonomous hybrid system in order to provide sufficient electrical energy supply for satisfying the stand-alone load demands at all times and conditions was proposed and considered. Optimal sizing and economical analysis of the hybrid system was accomplished using genetic algorithms for minimizing the annualized cost of system. A model of power-consumption for a microturbine was propounded and obtained using least square estimation algorithm based on capstone™ company data and was suggested for implementing at economic analysis. Less environmental pollution emission, less noise generation, less power fluctuation, more reliability and more fuel flexibility in comparison with a diesel generator cause that a microturbine was propounded as a back up for the hybrid system. Using synthetic operation of model reference adaptive control and feedback linearization technique, the maximum power and torque of the wind turbine were extracted and applied to the ISVC in the SEIG. In order to control the load voltage and frequency, a sinusoidal pulse width modulation method was used. For achieving the proper operation of the supervisory controller to adjust the reference power values of controllers correctly, the open circuit voltage estimation method for estimating the value of the SOC has been implemented. The supervisory controller has been used for the management of energy between generated and consumed energies. The proposed system can be used in the isolated rural and mountainous areas where are far from the power generation networks.

References

[1] Ackermann Thomas. Wind power in power system. John Wiley & Sons Press; 2005.
[2] Tabesh Ahmadreza, Iravani Reza. Small signal dynamic model and analysis of a fixed-speed wind farms-a frequency response approach. IEEE Trans Power Delivery 2006;21(2).
[3] Krichen Lotfi, Francois Bruno, Ouali Abderrazak. A fuzzy logic supervisory for active and reactive power control of a fixed speed wind energy conversion system. Electr Power Syst Res 2007.
[4] Tapia A, Tapia G, Ostolaza JX. Reactive power control of wind farms for voltage control applications. Renew Energy 2004.
[5] Thiriger Torbojorn, Linders J. Control by variable rotor speed of a fixed pitch wind turbine operation in a wide speed range. IEEE Trans Energy Convers 1993:520–6.
[6] De Almeida Rogerio G, Castronuovo Edgardo D, Lopes JA. Optimum generation control in wind parks when carrying out system operator request. IEEE Trans Power Syst 2006.
[7] Simoes Marcelo Godoy, Bose Bimal K, Spiegel Roland J. Fuzzy logic based intelligent control of a variable speed cage machine wind generation system. IEEE Trans Power Electron 1997;12(1).
[8] Hilloowala Robin M. Rule based fuzzy logic control for a PWM inverter in a standalone wind energy conversion scheme. IEEE Trans Indus Appl 1996:57–65.
[9] Chedid Zriad B, Karaki Sami H, El-Chamali Chadi. Adaptive fuzzy control for wind-diesel weak power system. IEEE Trans Energy Convers 2000;15(1).
[10] Tanaka T, Toumiya T. Output control by hill-climbing method for a small wind power generation system. Renew Energy 1997:389–400.
[11] Kamal Elkhatib et al. Int J Electr Power Energy Syst 2010:170–7.
[12] Nandi Sanjoy Kumar, Ghosh Himangshu Ranjan. A wind – PV battery hybrid power system at Sitakundain Bagladesh. Energy Policy 2009:3659–64.
[13] Dursun Erkan et al. Comparative evaluation of different power management strategies of a stand-alone PV/Wind/PEMFC hybrid power system. Int J Electr Power Energy Syst 2012:81–9.
[14] Hocaoglu Fatih O, Gerek Ömer N, Kurban Mehmet. A novel hybrid (wind–photovoltaic) system sizing procedure. Solar Energy 2009.
[15] Beyer Hans Georg, Langer Christian. A method for identification of configurations PV/wind hybrid systems for the reliable supply of small loads. Solar Energy 1996:381–91.
[16] Sebastian R. Modelling and simulation of a high penetration wind diesel system with battery storage. Int J Electr Power Energy Syst 2011:767–74.

[17] Tripathy SC, Kalantar M, Balasubramanian R. Dynamic and stability of wind and diesel turbine generators with superconducting magnetic energy storage unit on an isolated power system. IEEE Trans Energy Convers 1991:579–85.
[18] Das D, Aditya SK, Kothari DP. Dynamic of diesel and wind turbine generators on an isolated power system. Electr Power Energy Syst 1999:183–9.
[19] Salkind AJ, Fennie C, Singh P, Atwater T, Reisner DE. Determination of state of charge and state-of-health of batteries by fuzzy logic methodology. J Power Sources 1999;80:293–300.
[20] Cai CH, Du D, Liu ZY. Battery state-of-charge (SOC) estimation using adaptive neuro-fuzzy inference system (ANFIS). In: IEEE international conference on fuzzy system, USA; 2003. p. 1068–73.
[21] Pang S, Farrell J, Du J, Barth M. Battery state-of-charge estimation. In: IEEE American control conference, vol. 2; 2002. p. 1644–9.
[22] Yang Hongxing, Zhou Wei, Lu Lin, Fang Zhaohong. Optimal sizing method for stand-alone hybrid solar–wind system with LPSP technology by using genetic algorithm. Solar Energy 2008:354–67.
[23] Saheb-Koussa D, Haddadi M, Belhamel M. Economic and technical study of a hybrid system (wind-photovoltaic-diesel) for rural electrification in Algeria. Appl Energy 2009:1024–30.
[24] Dekker J et al. Economic analysis of PV/diesel hybrid power system in different climatic zones of South Africa. Int J Electr Power Energy Syst 2012;40:104–12.
[25] Roy Anindita, Kedare Shireesh B, Bandyopadhyay Santanu. Application of design space methodology for optimum sizing of wind–battery systems. Appl Energy 2009.
[26] Hongxing Yang, Wei Zhou, Chengzhi Lou. Optimal design and techno-economic analysis of a hybrid solar–wind power generation system. Appl Energy 2009:163–9.
[27] Diaf S, Notton G, Belhamel M, Haddadi M, Louche A. Design and techno-economical optimization for hybrid PV/wind system under various meteorological conditions. Appl Energy 2008:968–87.
[28] Alliant energy: Capstone™ MicroTurbine. <http://www.alliantenergy.com>.
[29] Durr Matthias, Cruden Andrew, Gair Sinclair, McDonald JR. Dynamic model of a lead acid battery for use in a domestic fuel cell system. J Power Sources 2006:1400–11.
[30] Singh SP. Self excited induction generator research – a survey. Electr Power Syst Res 2004:107–14.
[31] Masmoudi Ahmed. Stability analysis of the doubly fed machine with emphasis on saturation effects. COMPEL: Int J Comput Math Electr Electron Eng 2003;22(2):410–23.
[32] Lei Yazhou, Mullane Alan, Lightbody Gordon, Yacamini Robert. Modelling of the wind turbine with a doubly fed induction generator for grid integration studies. IEEE Trans Energy Convers 2006;21(1):257–64.
[33] Chan TF, Lai LL. An axial-flux permanent-magnet synchronous energy for a direct-coupled wind turbine system. IEEE Trans Energy Convers 2007;22(1).
[34] Ghedamsi K et al. Improvement of the performance for wind energy conversion systems. Int J Electr Power Energy Syst 2010:936–45.
[35] MunOng Chee. Modelling and dynamic simulation of electric machinery using Matlab/Simulink. Prentice Hall Press; 1998.
[36] Bose Bimal K. Modern power electronics and Ac drives. Prentice Hall Press; 2002.
[37] Adee Bruce H. Tidal power technology update, ppt format. University of Washington; 2007.
[38] Al-Hinai Amer, Feliachi Ali. Dynamic model of a microturbine used as a distributed generator. In: IEEE proceeding of the thirty-fourth southeaslern symposium on system theory; 2002. p. 209–13.
[39] Nikkhajoei Hassan, Reza Iravani M. A matrix converter based microturbine distributed generation system. IEEE Trans Power Delivery 2005;20(3).
[40] Li-Shrkht MY, Sisworahardjo NS, Uzunoglu M, Onar O, Alam MS. Dynamic behavior of PEM fuel cell and microturbine power plant. J Power Sources 2007:315–21.
[41] Nam Kwangghee, Arapostathis Aristol. A model reference adaptive control scheme for pure-feedback nonlinear systems. IEEE Trans Autom Control 1988;33(9).
[42] Boukhezzar B, Lupu L, Siguerdidjane H, Hand M. Multivariable control strategy for variable speed, variable pitch wind turbine. Renew Energy 2007:1273–87.
[43] Slotine E. Wiping, applied nonlinear control. Prentice Hall Press; 1991.
[44] Sebastian R, Quesada J. Distributed control system for frequency control in an isolated wind system. Renew Energy 2006:285–305.
[45] Mohan Ned, Undeland Tore M, Robbins William P. Power electronics: converters, applications and design. John Wiley& Sons press; 1995.